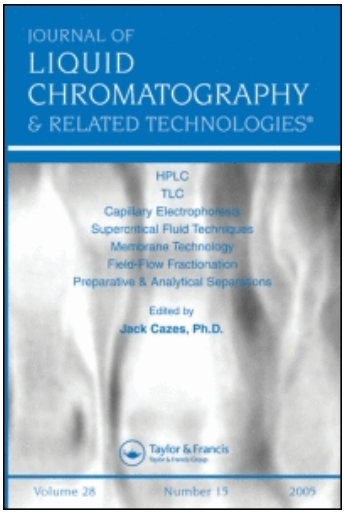

Journal of Liquid Chromatography & Related Technologies
Publication details, including instructions for authors and subscription information:
http://www.informaworld.com/smpp/title~content=t713597273

Micro-channel Thermal Field-Flow Fractionation: High-Speed Analysis of Colloidal Particles

Josef Janca[a]
[a] Pôle Sciences et Technologie, Université de La Rochelle, La Rochelle, Cedex 01, France

Online publication date: 03 December 2003

To cite this Article Janca, Josef(2003) 'Micro-channel Thermal Field-Flow Fractionation: High-Speed Analysis of Colloidal Particles', Journal of Liquid Chromatography & Related Technologies, 26: 6, 849 — 869
To link to this Article: DOI: 10.1081/JLC-120018888
URL: http://dx.doi.org/10.1081/JLC-120018888

MARCEL DEKKER, INC. • 270 MADISON AVENUE • NEW YORK, NY 10016

JOURNAL OF LIQUID CHROMATOGRAPHY & RELATED TECHNOLOGIES®
Vol. 26, No. 6, pp. 849–869, 2003

Micro-channel Thermal Field-Flow Fractionation: High-Speed Analysis of Colloidal Particles

Josef Janca*

Université de La Rochelle, Pôle Sciences et Technologie,
La Rochelle, France

ABSTRACT

Micro-thermal field-flow fractionation (μ-TFFF) was developed recently and applied for the characterization of the synthetic polymers and colloidal particles. In comparison with standard size TFFF channels, which were already used for the separation of the colloidal particles, the miniaturized channel allows one to shorten the time of the analysis and to achieve high resolution if the separation is performed under optimized experimental conditions. The relaxation processes leading to the establishment of the initial steady state after the injection of the sample into the channel can influence the retention and contribute to the zone broadening. These processes are considerably influenced by the temperature, which has to be carefully chosen. The choice of a convenient flow rate represents a

*Correspondence: Josef Janca, Université de La Rochelle, Pôle Sciences et Technologie, Avenue Michel Crépeau, 17042, La Rochelle Cedex 01, France; E-mail: jjanca@univ-lr.fr.

DOI: 10.1081/JLC-120018888 1082-6076 (Print); 1520-572X (Online)

compromise between an optimum flow rate (which is too slow due to the low diffusion coefficients of the colloidal particles) and a reasonable flow rate which takes into account the injection period and the stop-flow procedure applied immediately after the injection of the sample in order to minimize the effect of the relaxation processes. All these parameters can easily be optimized in the μ-TFFF due to its high versatility and to an important decrease of the heat energy flux across the channel, allowing an independent control of the temperatures of the cold and hot walls. The μ-TFFF thus becomes high-performance method for the separation of the colloidal particles and for the determination of their particle size distribution (PSD).

Key Words: Micro-thermal field flow fractionation; High-speed separation; Colloidal particles; Particle size-retention relationship; Injection-stop-flow time optimization.

INTRODUCTION

Micro-thermal field-flow fractionation (μ-TFFF) is a new technique developed recently[1,2] and applied, also, for the separation of colloidal particles.[2] The standard size TFFF channels were extensively used during the last few years to investigate the behavior of the colloidal particles,[3–12] but no study was oriented towards the optimization of the experimental conditions. The state of the art concerning the applications of various FFF techniques for the separation of the colloidal particles was reviewed recently.[13] However, a fundamental study is necessary in order to optimize the experimental conditions of the μ-TFFF and thus to exploit, fully, all advantages of this new technique.

With regard to the advantages of the μ-TFFF, it is necessary to mention a paper[14] describing the construction of a channel with the use of the materials of low thermal conductivity in which the high temperature difference of 46 K measured outside the channel must be established to obtain as low effective temperature drop as 4.8 K while much higher temperature drop is necessary to fractionate small colloidal particles and macromolecules.

Although only very few experiments were presented in the paper,[14] it is difficult to understand some of them. The elution time of the unretained solute given in Fig. 6, Ref.[14], is shorter at lower temperature drop compared with the values given in Fig. 7, Ref.[14]. This might be caused by an important thermal dilation of the channel under the various experimental conditions, which represents a serious drawback of its construction.

When calculating the experimental plate heights, H, by using the fractogram in Fig. 7, Ref.[14], and the well-known relationship:

$$H = L\left(\frac{\sigma}{V_R}\right)^2 \tag{1}$$

where L is the length of the channel, V_R is the retention volume of the concerned solute, and σ is the standard deviation characterizing the width of the fractogram in the same volume units as V_R, the plate height calculated for the unretained solute is $H = 0.93$ cm. With respect to the elution time of 31.2 s of this unretained solute and the given flow rate of 1.25 mL/h, the only possible dimensions of the separation channel in the described experiment are 27 μm × 6 mm × 6.5 cm. Thus, the linear velocity of the carrier liquid was $\langle v \rangle = 0.214$ cm/s. On the other band, the plate height corresponding to the $\langle v \rangle = 0.214$ cm/s, taken from Fig. 5, Ref.[14], is roughly $H = 1.2$ cm. The origin of the important difference, compared with the above calculated $H = 0.93$ cm, is not clear. The fractogram in Fig. 7, Ref.[14] is assumed by the authors to represent a separation of two different size colloidal samples. This cannot be true because the "separated" peaks are narrower than the void volume peak, but such a result is theoretically impossible[15,16] and the known experimental FFF data[17] generally confirmed the theory.

When neglecting the contribution of the longitudinal diffusion and of the extra-channel elements to the zone broadening, the approximate relationship[15] for the plate height H, based on the theory of the zone broadening in FFF, combined with the well-known Stokes–Einstein relationship for the diffusion coefficient of a suspension of the hard spherical particles, can be written as:

$$H = \frac{\chi w^2 \langle v \rangle}{D} = \frac{2R^3 w^2 \langle v \rangle \pi \eta r_p}{3k_B T} \tag{2}$$

where R is the retention ratio and χ is the dimensionless parameter, both defined below, w is the thickness of the channel, $\langle v \rangle$ is the average linear velocity of the carrier liquid, r_p is the particle radius, k_B is Boltzmann constant, η is the viscosity of the carrier liquid, and T is the temperature. A simple calculation with the use of the Eq. (2) and of the experimental data given in Ref.[14], namely $w = 27$ μm, $\langle v \rangle = 0.214$ cm/s, $T = 297$K (cold wall temperature), $\eta = 0.0094$ Poise for water at 297K, and the retention ratios $R_1 = 0.441, R_2 = 0.312$, corresponding to the peaks of the retained particles 204 and 272 nm in Fig. 7, Ref.[14], provides the plate heights $H_{1,\text{theor}} = 0.654$ cm and $H_{2,\text{theor}} = 0.309$ cm, respectively. On the other hand, the experimental plate heights calculated from the fractogram in Fig. 7,

Ref.[14] by using Eq. (1), are $H_{1,\mathrm{exp}} = 0.017\,\mathrm{cm}$ and $H_{2,\mathrm{exp}} = 0.0021\,\mathrm{cm}$, respectively. The experimental dependence of the plate height on the linear velocity in Fig. 5, Ref.[14] shows, clearly, that the efficiency of the described separation system measured by the plate height is largely below the theoretical values. Consequently, by taking into account the theory, the retained peaks in Fig. 7, Ref.[14] should be at least 6.5× and 13× larger, respectively, and unresolved even if the particle size distribution (PSD) of both samples is completely neglected. As a result, it seems that the supposed separation in Fig. 7, Ref.[14] is an artifact and not a useful extension of the FFF miniaturization trends.[18]

Another goal of this study was, then, to prove that high performance and high-speed separation of the colloidal particles can be achieved in a μ-TFFF channel, provided its construction is optimized, the experiments are carried out correctly under the appropriate experimental conditions, and the results are interpreted accurately.

THEORY

A crucial characteristic of colloidal particles is the low diffusion coefficient, D, related to their size by the Stokes–Einstein relationship whenever the particles in a suspension can be considered as hard non-interacting spheres:

$$D = \frac{k_{\mathrm{B}}T}{6\pi\eta r_p} \tag{3}$$

The theoretical optimum average linear velocity of the carrier liquid is related to the diffusion coefficient by:[1]

$$\langle v\rangle_{\mathrm{opt}} = \frac{D}{w}\sqrt{\frac{2}{\chi R}} \tag{4}$$

The retention ratio, R, is given by:[15]

$$R = 6\lambda\left[\coth\left(\frac{1}{2\lambda}\right) - 2\lambda\right] = \frac{V_0}{V_R} \tag{5}$$

where V_0 is the elution volume of an unretained species, V_R is the retention volume of a retained species, and $\lambda = \ell/w$, where ℓ is a distance between the accumulation wall and the center of gravity of the steady-state concentration

distribution across the channel of the retained species. It holds for highly retained species:

$$\lim_{\lambda \to 0} R = 6\lambda \tag{6}$$

Equations (5) and (6) describe, rigorously, the retention only if a parabolic flow velocity profile is formed inside the channel. Such a condition is not fulfilled in TFFF, due to the viscosity variation with the temperature across the channel. The retention ratio, taking into account a non-parabolic flow velocity profile, is:[19]

$$R_{\mathrm{np}} = 6\lambda k(1 - R) + R \tag{7}$$

where k is a constant whose value is determined by the properties of the carrier liquid, the cold wall temperature, and the field strength, and R is the retention ratio under the conditions of isoviscous flow. By neglecting the term with square of λ, it holds:

$$\lim_{\lambda \to 0} R_{\mathrm{np}} = 6\lambda(1 + k) \tag{8}$$

The errors resulting from this approximation do not exceed the experimental uncertainty of the μ-TFFF data for highly retained species. It holds for χ:[20]

$$\chi = \frac{24\lambda^3}{1 + \exp(-1/\lambda) - 2\lambda[1 - \exp(-1/\lambda)]} B \tag{9}$$

where

$$B = (28\lambda^2 + 1)\left[1 - \exp\left(\frac{-1}{\lambda}\right)\right] - 10\lambda\left[\exp\left(\frac{-1}{\lambda}\right) + 1\right] - \frac{1}{3\lambda^2} - \frac{2}{\lambda} + 4 - \frac{1/\lambda}{1 - \exp(-1/\lambda)}\left\{4\lambda\left[1 + \frac{1/\lambda}{1 - \exp(-1/\lambda)}\right] - \frac{1}{3\lambda} - 6\right\} \tag{10}$$

The dependence of the optimum average velocity of the carrier liquid on the diameter of the retained colloidal particles, calculated by using the above Eq. (3)–(6) and (9) is demonstrated in the Fig. 1 for two different λ values, representing the limits of practically useful retentions. Obviously, the optimum velocities are too low for practical experimental work. Thus, the question is how far from an optimum velocity an acceptable resolution can be achieved in a reasonable time?

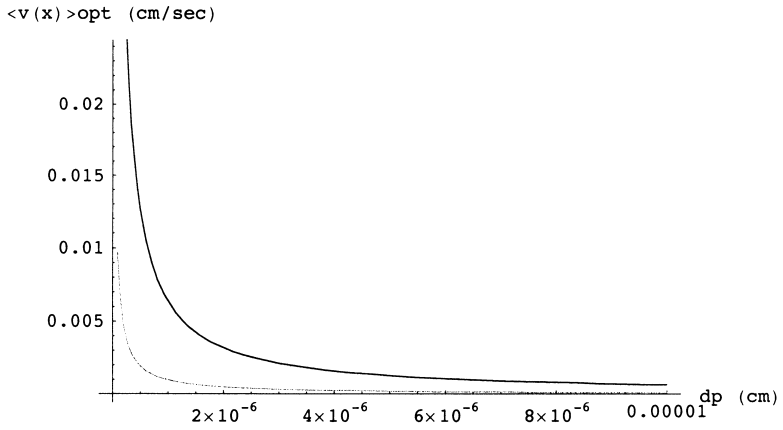

Figure 1. Dependence of the optimum average linear velocity of the carrier liquid on the diameter of the retained colloidal particles calculated from Eqs. (3) and (4). Black curve corresponds to $\lambda = 0.4$, $R = 0.909$, and grey curve to $\lambda = 0.01$, $R = 0.059$; $w = 0.005$ cm, $\eta_{\text{water}} = 0.01$ cp.

The linear velocities in standard size TFFF of colloidal particles lie in the range from 0.02 to 0.3 cm/s, which are 20 to 300 times higher than the optimum values for weakly retained species and much higher for highly retained species (see Fig. 1). The time of the separation in these cases varies from 20 to 60 min. Under such conditions, the plate height is given correctly by Eq. (2) and the resolution, R_S, between two retained species 1 and 2 is given by:[1]

$$R_S = \left(\frac{\sqrt{L}}{2w\sqrt{\langle v\rangle}}\right)\left[\frac{|1/R_1 - 1/R_2|}{\left(\sqrt{\chi_1/D_1}/R_1 + \sqrt{\chi_2/D_2}/R_2\right)}\right] \tag{11}$$

As a result, the shortening of the channel accompanied by a proportional decrease of the average velocity $\langle v\rangle$ will keep the resolution unchanged. On the other hand, no time economy can be achieved. Nevertheless, we have shown[21] that an important shortening of the separation time can be achieved by a special injection–relaxation–elution procedure which consists of an injection of the sample at a slow flow rate followed by a stop-flow period for the relaxation, and then by the elution at higher flow rate. Under such conditions, the resolution is the same but the time of the separation is shorter, compared with the other mode of the injection–relaxation carried out at the identical flow rates during the injection and elution after the stop-flow period. On the other hand, it is necessary to avoid the perturbations due to the

hydrodynamic lift forces[22] emerging at high flow rates and due to the steric exclusion mechanism,[23] which can appear if the temperature drop is too high. Both effects complicate the separation.

A steady-state concentration distribution of the retained species is usually not reached during, or immediately after, the injection of the sample into the channel. The retained species migrate across the channel from the depletion to the accumulation wall due to the field action and, simultaneously, along the channel due to the flow. Consequently, the zone of the retained species is broader compared with a theoretical zone eluted under steady-state conditions. In order to avoid this additional zone broadening, the flow rate of the carrier liquid should be reduced during the injection and casually stopped after the injection for a time necessary to establish a steady-state concentration distribution across the channel. Such a relaxation time can be calculated as:[21]

$$t_\varepsilon = \frac{w^2 F(\lambda)}{D} \tag{12}$$

where

$$F(\lambda) = -\frac{1}{\pi^2 U(\lambda)} \ln\left\{\frac{\pi^2 U(\lambda)\varepsilon}{4[1+\cosh(1/2\lambda)]}\right\} \tag{13}$$

$$U(\lambda) = 1 + \frac{1}{4\pi^2\lambda^2} \tag{14}$$

The ε is the relative deviation of the concentration difference Δc_t between $x = 0$ and $x = w$ at the time t from the Δc_{SS} in a steady state:

$$\varepsilon = \frac{\Delta c_{SS} - \Delta c_t}{\Delta c_{SS}} \tag{15}$$

The calculation of the relaxation time t_ε is based on a rigorous theoretical model of the settling of small particles in a fluid, which was published by Mason and Weaver[24] in 1924, developed further by Weaver,[25] and finalized by Van Holde and Baldwin[26] in 1958. Later on, Hovingh et al.[15] proposed another relationship to calculate the relaxation time, t_r:

$$t_r = \frac{w^2\lambda}{D}\left\{\frac{1}{2} - \lambda + \left[\exp\left(\frac{1}{\lambda}\right) - 1\right]^{-1}\right\} \tag{16}$$

which was simplified[27] to obtain:

$$t_r = \frac{w^2 \lambda}{D} \tag{17}$$

A comparison of the above theoretical approaches is shown in Fig. 2, which represents the dependences of the relaxation time on the retention parameter λ, calculated by using the input data corresponding to the experiments carried out in this work. The black and grey curves in Fig. 2 correspond to the model described by the Eq. (12)–(15) with the respective deviations from the equilibrium $\varepsilon = 1$ and 5%, while the straight-line corresponds to the Eq. (17). Equation (16) is represented by the lowest dashed curve in Fig. 2. Kirkland et al.[28] studied, experimentally, the stop-flow time necessary to obtain the retentions not influenced by the relaxation processes in Sedimentation FFF. They have found that the actual stop-flow times were much longer than those calculated from the Eq. (13). Although we have studied the applicability of the above theoretical approaches in the Sedimentation FFF of colloidal particles,[21] they should be directly applicable to the μ-TFFF as well. Thus, the principal goal of this work was to optimize the experimental conditions of the μ-TFFF with respect to the injection–relaxation–elution procedure, in order to achieve high-resolution, high-speed, separation of the colloidal particles.

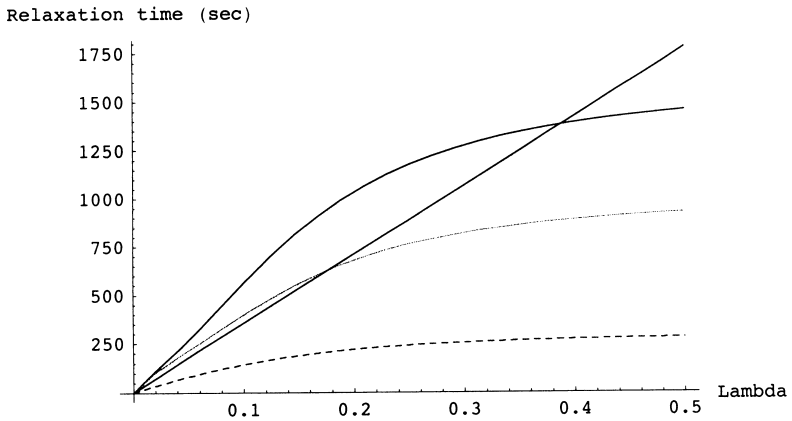

Figure 2. Dependence of the relaxation time on the λ. Input data: dp = 155 nm, $w = 0.01$ cm. Black curve is calculated from Eq. (12), for $\varepsilon = 0.01$, the grey curve from Eq. (12) for $\varepsilon = 0.05$. Dashed curve is calculated from Eq. (16) and the straight-line is calculated from Eq. (17).

Table 1. Particle sizes of polystyrene latexes.

Polystyrene latex	Diameter (nm)	Standard deviation (nm)
	Supplier's data	
PSL 60	60 ± 2.5	not given
PSL 155	155 ± 4	not given
PSL 343	343 ± 9	not given
μ-TFFF data at flow rate of 10 μL/min $\Delta T = 19$K, $T_c = 292$K		
PSL 60	61	23
PSL 155	156	54
PSL 343	341	75
μ-TFFF data at a flow rate of 20 μL/min $\Delta T = 27$K, $T_c = 297$K		
PSL 155	157	59
μ-TFFF data at a flow rate of 60 μL/min $\Delta T = 32$K, $T_c = 315$K, 10 μL/min during injection, 1 min stop-flow		
PSL 155	155	55

EXPERIMENTAL

The μ-TFFF channel was previously described in detail.[1] The temperature of the cold wall was kept constant by using a low temperature thermostat, Model RML 6 B, (Lauda, Germany). The electric power for the heating cartridge was regulated by an electronic variac to control the temperature of the hot wall. Both temperatures were measured with a digital thermometer (Hanna Instruments, Portugal) equipped with two thermocouples.

The polystyrene latex (PSL) particles (Duke Scientific Corp., USA) were used as model samples. Their particle sizes are given in Table 1. The aqueous solution of 0.1% detergent Brij 78 (Fluka, Germany) and of 0.02% of NaCl was used as a carrier liquid.

RESULTS AND DISCUSSION

Size Dependence of the Retention

The thermal diffusion of the colloidal particles is a complex phenomenon[29–31] because the interactions between the suspended particles and the components of the carrier liquid influence not only the magnitude of the thermal diffusion coefficients, but also its sign, especially when the carrier liquid is a mixed solvent. As far as these phenomena are not yet well

understood, the full potential and performance of the μ-TFFF in the field of the separation of the colloidal particles are difficult to evaluate. The retention parameter λ is related to the size of the fractionated particles by:

$$\lambda = \frac{k_B T}{6\pi\eta r D_T \Delta T} \tag{18}$$

which results from the basic relationship:

$$\lambda = \frac{D}{D_T \Delta T} \tag{19}$$

combined with the Eq. (1), where D_T is the thermal diffusion coefficient. Although, as mentioned above, the dependence of the thermal diffusion coefficient on the size and chemical nature of the colloidal particles is not yet theoretically well understood, it exists and it varies with the experimental conditions as demonstrated experimentally.[5,12] Nevertheless, it is clear that, at least in those cases when this dependence is weak or zero, the size selectivity of the TEFF is comparable to Flow FFF for which $\lambda = k_{FFFF}/r$ (where k_{FFFF} is a constant for given experimental conditions of Flow FFF). Consequently, μ-TFFF can become an interesting means not only for the fundamental studies of the thermal diffusion of colloidal particles, but also a powerful technique of PSD analysis, besides its well established applications in the field of polymer characterization. The expected linear dependence of the retention parameter λ on the reciprocal value of the particle size, given by Eq. (18), was found for the μ-TFFF of the polystyrene latices separated under the given experimental conditions and is shown in Fig. 3.

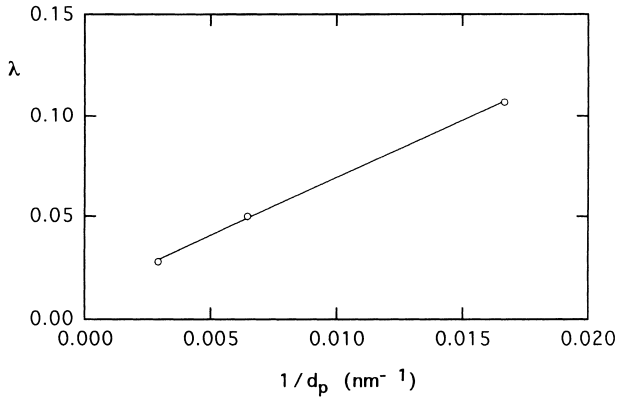

Figure 3. Dependence of the retention parameter λ on the reciprocal value of the particle diameter for given experimental conditions of the μ-TFFF. Experimental conditions: flow rate 10 μL/min, $\Delta T = 18$K, cold wall temperature 292K.

Effect of the Stop-Flow Time

As pointed out above, an important increase of the resolution in μ-TFFF (as in any other FFF technique) can be achieved by optimizing the sample injection and stop-flow procedures. We have chosen, for this demonstration, the polystyrene latex of an intermediate size; however, the identical experimental results were found independent of the size of the studied sample.

A positive impact of the stop-flow period following the injection of the sample into the channel is shown in Fig. 4. When the flow rate in the μ-TFFF experiment was increased from 10–20 μL/min, not only the width of the peak increased due to the relaxation and dispersive processes, but also its maximum shifted to lower retention volume due to the increased amount of the unrelaxed species. Even an important peak appeared corresponding to the unrelaxed species eluted with higher than the average flow velocity. Such a peak was practically negligible at the flow rate 10 μL/min.

The next fractograms show that, whenever the short injection lasting a few seconds for full introduction of the sample into the channel was followed by a stop-flow period, the maximum of the peak appeared at the same retention volume as at the flow rate 10 μL/min and the relaxation peak was substantially reduced. The stop-flow time of 1 min was apparently long enough, under the given experimental conditions, to minimize the effect of the relaxation phenomena. A further increase of the stop-flow time to 3 and 6 min had not a significant effect on the position, width, and the whole shape of the fractogram. This experimental stop-flow time lies between the theoretical relaxation times calculated from the Eqs. (12) and (16) and shown in Fig. 2 for the corresponding $\lambda = 0.05$; however, it is closer to the result obtained from Eq. (16).

A better agreement with Eq. (12) can be obtained for a higher value of ε. Figure 5, representing the dependence of the relaxation time on the ε calculated from Eq. (12) for the $\lambda = 0.05$, shows that the departure from the steady state after the stop-flow period should be as high as $\varepsilon = 0.5$ to obtain a satisfactory agreement of the experiment with the theory. Nevertheless, it seems unrealistic to obtain the same retention and the width of the fractogram under such conditions, in comparison with steady-state conditions established from the very beginning of the elution.

The results of the above comparison of the experiments with various theoretical models of relaxation processes merit a more detailed analysis of the postulates of the theories. As a matter of fact, the model developed by Hovingh et al.[15] is based on an *a priori* assumption that the relaxation time is the average time of travel of the retained species from the center of the channel $x = w/2$ to the steady-state center of gravity of the concentration distribution across the channel. This travel distance was chosen arbitrarily, even if one can suppose implicitly that the species at the depletion wall can reach their steady-state positions at the same time.

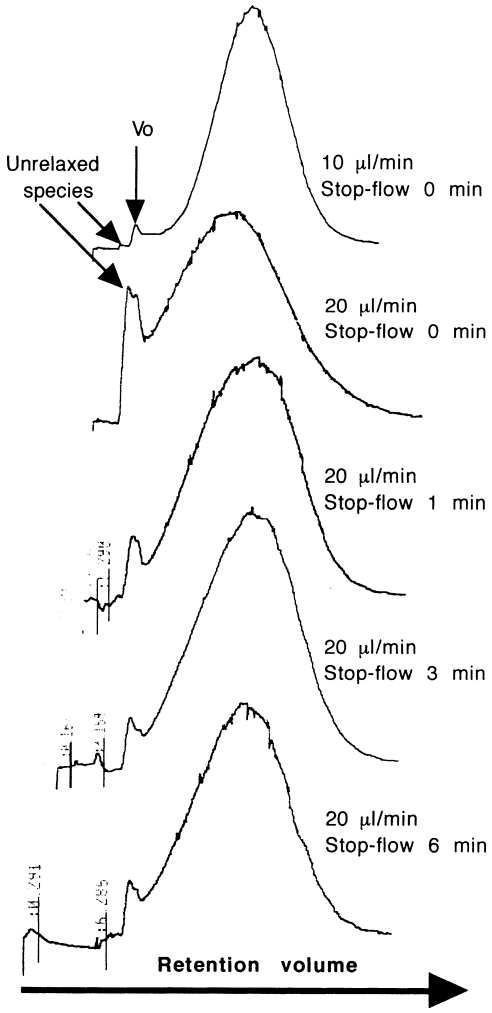

Figure 4. Fractograms demonstrating the effect of the flow rate and stop-flow time. Experimental conditions: $\Delta T = 19$K, cold wall temperature 292K.

As concerns Eq. (17), it is obtained by substituting the term within the brackets in Eq. (16) by 1, which gives to the relaxation time the physical meaning of the travel time of a retained species from the depletion to the accumulation wall. This is, of course, an arbitrary choice.

Physically, the most rigorous model of Mason and Weaver[24] is based on the calculation of the relaxation time as a function of the departure from the

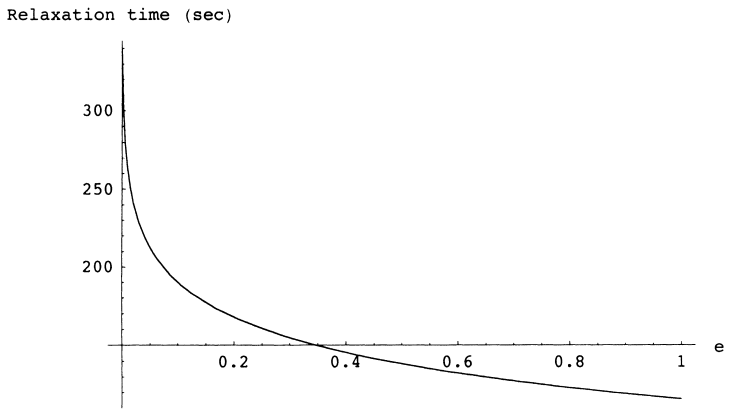

Figure 5. The relaxation time as a function of the departure from the steady state ε. Input data $d_p = 155$ nm, $w = 0.01$ cm, $\lambda = 0.05$.

steady state. The ratio $F(\lambda)/\lambda$, which is a measure of the agreement between the relaxation time calculated either from Eq. (12) or (17) can, coincidentally, approach to one, for some values of λ and ε, as demonstrated previously.[21]

The important difficulties concerning the comparison of any theoretical model with the experiments are that the sample injected at the beginning of the channel is far from a uniform concentration distribution within the occupied volume, due to the synergism of the flow velocity distribution across the channel, not negligible flow velocity distribution in a plane parallel to the accumulation and depletion walls, which is caused by the tapered entry of the channel and, finally, due to the migration of the retained species towards the accumulation wall from the very beginning of the injection. Consequently, the exact spatial concentration distribution of the injected zone at the beginning of the stop-flow period is very complicated and is not known. Moreover, it is difficult to estimate to which degree of the departure from the steady state ε the relaxation should progress during the stop-flow time in order to reduce the effect of the relaxation phenomena on the retention and broadening of the zone below the limits of experimental errors of the measurement.

None of the theoretical models considers the complexity of the transport processes taking place during the injection. The only realistic solution could be found by a numerical simulation using a finite element method. However, we have shown, previously,[21] that an important suppression of the effect of the relaxation phenomena can be achieved by reducing the flow rate during the injection. As the injection time is very short, the whole time of the fractiona-

tion is not influenced in an important manner. This procedure was tested for the μ-TFFF and the results are described in the following text.

Effect of the Temperature

It has been observed, recently,[32] that the temperature has an important effect on the retention and dispersion or, generally, on the transport phenomena in μ-TFFF. Although the effect of the temperature is very complex, we have chosen to study, in this work, only the combined influence of the temperature and stop-flow procedure on the zone broadening of the retained species within the range of the cold wall temperatures at which the retention remains unchanged. The results are demonstrated in Fig. 6.

In comparison with the experiments shown in Fig. 4, the temperature drop ΔT was higher and this resulted in higher retention and lower zone broadening of the same PSL sample. As can be seen in Fig. 6, an increase of the cold wall temperature results in a small decrease of the zone width at the same flow rate 20 μL/min. The increase of the flow rate to 40 μL/min at this higher cold wall temperature leads to higher zone broadening, which is not reduced by stopping the flow during 1 min. On the other hand, further increase of the cold wall temperature to 323K results in a fractogram whose position and width are the same as at lower flow rate of 20 μL/min and lower cold wall temperature of 297K. Further increase of the cold wall temperature did not result in an additional decrease of the zone broadening. When increasing the flow rate to 50 μL/min, the zone broadening increases, the relaxation peak appears, and the application of 1 min of stop-flow did not change the observed decrease of the performance of the fractionation, as can be seen in Fig. 7.

Effect of the Reduced Flow Rate During the Injection

As mentioned above, an important increase of the efficiency of Sedimentation FFF was observed[21] when the flow rate during the injection of the sample was lower than that applied during the elution after the stop-flow period. The same operational procedure was tested in μ-TFFF and the results are shown in Fig. 8.

The flow rate during the injection (which lasted 10 s for the full introduction of 1 μL of the sample into the channel) was, in all cases, 10 μL/min followed by a stop-flow period and then by elution at a higher flow rate indicated on the fractograms. It can be seen, in Fig. 8, that an excellent fractionation was obtained when the stop-flow time was 1 min and the elution flow rate was 60 μL/min. The total analysis time was 15 min in this case. The increase of the elution flow rate to 200 μL/min with the same stop-flow time of 1 min leads to some deterioration of the separation; the total

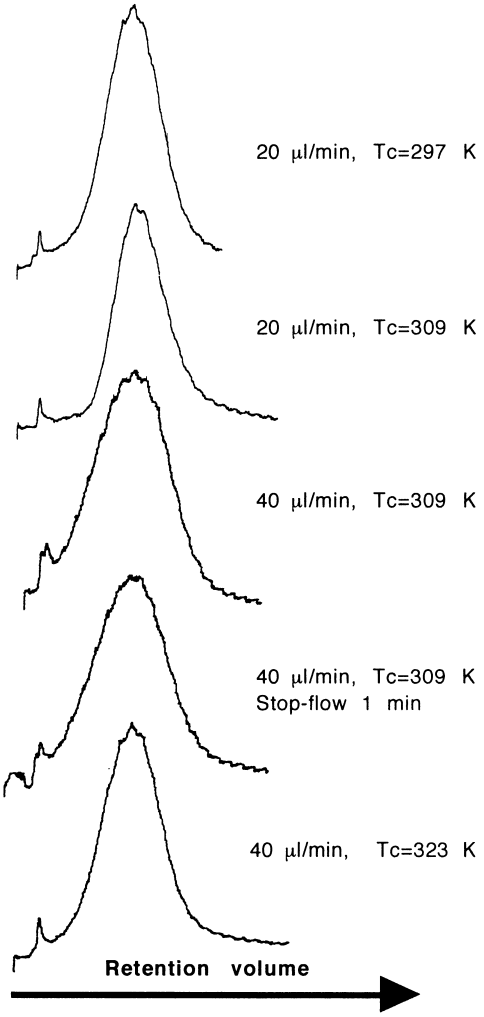

Figure 6. Fractograms demonstrating the effect of the temperature, flow rate, and stop-flow time. Experimental conditions: $\Delta T = 27$K.

analysis time was slightly shorter, i.e., 12 min. The prolongation of the stop-flow time to 2 min under otherwise identical operational conditions resulted in a good separation in 13 min. However, it can be seen, in Fig. 8, that some part of the sample was not ideally relaxed at the beginning of the fractionation and this resulted in an occurrence of the relaxation peak and in some broadening of

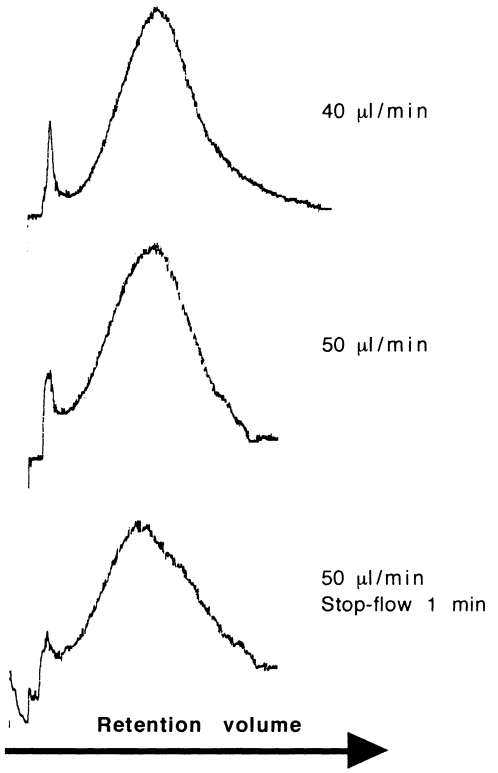

Figure 7. Fractograms demonstrating the effect of the medium flow rate and stop-flow time at higher cold wall temperature and higher temperature drop. Experimental conditions: $\Delta T = 32$K, cold wall temperature 315K.

the retained sample zone. Further increase of the elution flow rate to 300 μL/min resulted in an important shift of the peak maximum, broadening of the retained zone, and the occurrence of an important peak corresponding to the unrelaxed part of the sample. The total time of the fractionation was 10 min. The further prolongation of the stop-flow time was not reasonable because, even if the resolution might be slightly better, such operational procedure cannot lead to a shortening of the total analysis time. The progressive shift of the peak towards lower retention volume with increasing flow rate can be caused by a contribution of the lift forces. We have observed similar dependence of the retention on the flow rate in Sedimentation FFF of the colloidal PSL of a comparable size and within the same range of average linear velocities of the carrier liquid.[33]

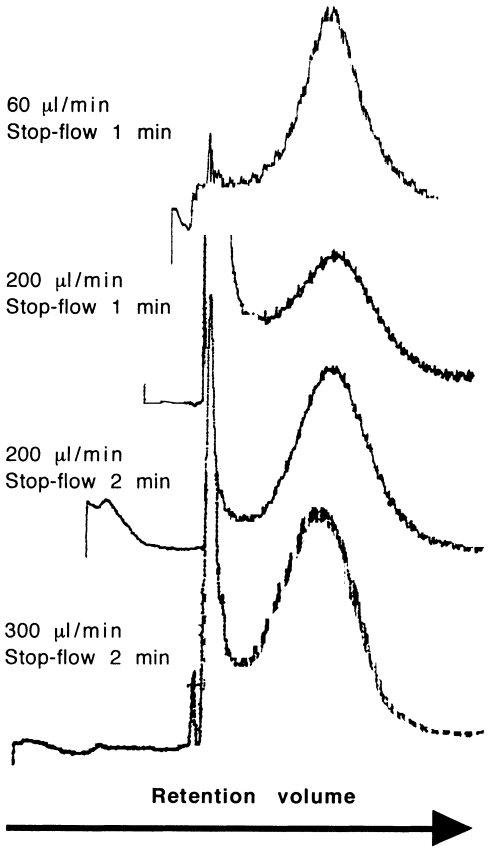

Figure 8. Fractograms demonstrating the effect of the high flow rate and stop-flow time at low flow rate during the injection. Experimental conditions: $\Delta T = 32$K, cold wall temperature 315K, flow rate during the injection 10 μL/min.

Determination of Particle Size Distribution

The fractograms from the μ-TFFF can be used to calculate the PSD of the separated colloidal samples. A detailed methodology, convenient for any FFF technique, was described recently[13] and a comparative study proved an excellent agreement between the average particle sizes and standard deviations of the PSD provided by the manufacturer of the PSL and the data obtained by Quasi-Elastic Light Scattering (QELS) and μ-TFFF.[2] The previous results were obtained at a low flow rate. It was, thus, interesting to check the performance of the μ-TFFF carried out under the optimized operational

conditions allowing high-speed fractionation. The results of the determination of the PSD, given in Table 1, demonstrate that the average particle diameters and the standard deviations of the PSD obtained from the μ-TFFF carried out under different but optimized experimental conditions are very close each to other, practically within the range of the experimental errors. As a result, the μ-TFFF is a high-performance high-speed method, allowing very precise determination of the PSD of colloidal particles. Its size selectivity is higher in comparison with QELS and the separation time is comparable to, or shorter than, the time necessary for the PSD analysis of one sample by the QELS; the total volume of a diluted sample necessary for one separation and analysis is very small, only 1 μL.

CONCLUSIONS

Micro-thermal field-flow fractionation is a very convenient high-speed and high-performance method for the separation of submicron colloidal particles and for the determination of their PSD. However, it is necessary to optimize the operational conditions in order to obtain accurate results, as well as to reduce the time of the fractionation.

The application of the stop-flow time after the injection of the separated sample is absolutely necessary if the flow rate during the whole separation run is relatively high. An increase of the average linear velocity, for example, from 0.033 to 0.066 cm/s, leads to an important increase of the zone broadening of the retained species and to the appearance of the relaxation peak in continuous elution operation without stopping the flow after the injection. Such a deterioration of the separation practically disappeared when the flow was stopped for a time long enough after the injection to allow the establishment of a nearly steady-state concentration distribution of the retained sample components before the elution.

The increased temperature has a positive effect on the acceleration of the relaxation phenomena. This phenomenon is under detailed study, which will be published soon.

The most important contributions to the zone broadening, to the peak shift, and to the emergence of the relaxation peak, which are caused by the relaxation processes, appear during the injection because the concentration distribution of the retained species is at its initial stage which is farthest from the steady state. Thus, all inconvenient consequences of the relaxation phenomena are most efficiently minimized by lowering the flow rate during the injection before the stop-flow period. This injection-stop-flow mode allows an important increase of the flow rate during the subsequent elution without losing the performance of the fractionation. As a result, high-performance

fractionation is obtained in shorter time. The μ-TFFF has a full potential to become highly competitive method for PSD analysis.

REFERENCES

1. Janca, J. J. Micro-channel thermal field-flow fractionation: new challenge in analysis of macromolecules and particles. Liq. Chrom. & Rel. Technol. **2002**, *25*, 683.
2. Janca, J. J. Micro-channel thermal field-flow fractionation: analysis of ultra-high molar mass polymers and colloidal particles with constant and programmed field force operation. Liq. Chrom. & Rel. Technol. **2002**, *25*, 2173.
3. Liu, G.; Giddings, J.C. Separation of particles in nonaqueous suspensions by thermal-electrical field-flow fractionation. Anal. Chem. **1991**, *63*, 296.
4. Liu, G.; Giddings, J.C. Separation of particles in aqueous suspensions by thermal field-flow fractionation. Measurement of thermal diffusion coefficients. Chromatographia **1992**, *34*, 483.
5. Shiundu, P.M.; Liu, G.; Giddings, J.C. Separation of particles in non-aqueous suspensions by thermal field-flow fractionation. Anal. Chem. **1995**, *67*, 2705.
6. Shiundu, P.M.; Giddings, J.C. Influence of bulk and surface composition on the retention of colloidal particles in thermal field-flow fractionation. J. Chromatogr. **1995**, *715*, 117.
7. Ratanathanawongs, S.K.; Shiundu, P.M.; Giddings, J.C. Size and compositional studies of core-shell latexes using flow and thermal field-flow fractionation. Colloids Surf. A Physicochem. Eng. Aspects **1995**, *105*, 243.
8. Giddings, J.C.; Shiundu, P.M.; Semenov, S.N. Thermophoresis of metal particles in a liquid. J. Colloid. Interf. Sci. **1995**, *176*, 454.
9. Jeon, S.J.; Schimpf, M.E. Separation of particles based on surface composition by thermal field-flow fractionation. Polym. Mater. Sci. Eng. **1996**, *75*, 4.
10. Van Batten, C.; Hoyos, M.; Martin, M. Thermal field-flow fractionation of colloidal materials: methylmethacrylate-styrene linear Di-Block copolymers. Chromatographia **1997**, *45*, 121.
11. Jeon, S.J.; Schimpf, M.E.; Nyborg, A. Compositional effects in the retention of colloids by thermal field-flow fractionation. A. Anal. Chem. **1997**, *69*, 3442.
12. Mes, E.P.C.; Tijssen, R.; Kok, W.Th. Influence of the carrier composition on thermal field-flow fractionation for the characterization of sub-micron polystyrene latex particles. J. Chromatogr. A **2001**, *907*, 201.

13. Janca, J. Field-flow fractionation in particle size analysis. In *Encyclopedia of Analytical Chemistry*; Myers, R.A., Ed.; J. Wiley & Sons: Chichester, 2000.
14. Edwards, T.L.; Gale, B.K.; Frazier, A.B. A microfabricated thermal field-flow fractionation system. Anal. Chem. **2002**, *74*, 1211.
15. Hovingh, M.E.; Thompson, G.M.; Giddings, J.C. Column parameters in thermal field-flow fractionation. Anal. Chem. **1970**, *42*, 195.
16. Giddings, J.C.; Chang, J.P.; Myers, M.N.; Davis, J.M.; Caldwell, K.D. Capillary liquid chromatography in field-flow fractionation-type channels. J. chromatogr. J. Chromatogr. **1983**, *255*, 359.
17. Janca, J. *Field-Flow Fractionation: Analysis of Macromolecules and Particles*; Marcel Dekker, Inc.: New York, 1988.
18. Schimpf, M.E. Polymer analysis by thermal field-flow fractionation. J. Liq. Chrom. & Rel. Technol. **2002**, *25*, 2101.
19. Brimhall, S.L.; Myers, M.N.; Caldwell, K.D.; Giddings, J.C. Study of temperature dependence of thermal diffusion in polystyrene/ethylbenzene by thermal field-flow fractionation. J. Polym. Sci., Polym. Phys. Ed. **1985**, *23*, 2443.
20. Giddings, J.C.; Yoon, Y.H.; Caldwell, K.D.; Myers, M.N.; Hovingh, M.E. Nonequilibrium plate height for field-flow fractionation in ideal parallel plate columns. Separ. Sci. **1975**, *10*, 447.
21. Janca, J.; Chmelik, J.; Pribylova, D. Optimization of field-flow fractionation with respect to relaxation and use of stop-flow technique at constant field operation. J. Liq. Chrom. **1985**, *8*, 2343.
22. Caldwell, K.D.; Nguyen, T.T.; Myers, M.N.; Giddings, J.C. Observations on anomalous retention in steric Field-flow fractionation. Sep. Sci. Technol. **1979**, *14*, 935.
23. Giddings, J.C. Displacement and dispersion of particles of finite size in flow channels with lateral forces. Field-flow fractionation and hydrodynamic chromatography. Sep. Sci. Technol. **1978**, *13*, 241.
24. Mason, M.; Weaver, W. The settling of small particles in a fluid. Phys. Rev. **1924**, *24*, 412.
25. Weaver, W. The duration of the transient state in the settling of small particles. Phys. Rev. **1926**, *27*, 499.
26. Van Holde, K.E.; Baldwin, R.L. Rapid attainment of sedimentation equilibrium. J. Phys. Chem. **1958**, *62*, 734.
27. Giddings, J.C.; Karaiskakis, O.; Caldwell, K.D. Concentration and analysis of dilute colloidal samples by sedimentation FFF. Sep. Sci. Technol. **1981**, *16*, 725.
28. Kirkland, J.J.; Yau, W.W.; Doemer, W.A.; Grant, J.W. Sedimentation field-flow fractionation in macromolecule characterization. Anal. Chem. **1980**, *52*, 1944.

29. Semenov, S.N. Thermophoresis and thermal FFF of particles in electrolytes. J. Microcol. Sep. **1997**, *9*, 287.
30. Semenov, S.N. Surface phenomena in thermal FFF of particles. J. Liq. Chromatogr. & Rel. Technol. **1997**, *20*, 2687.
31. Morozov, K.I. On the theory of soret effect in colloids. In *Thermal Nonequilibrium Phenomena in Fluid Mixtures*; Koehler, W., Wiegand, S., Eds.; Lecture Notes in Physics; Springer: 2002.
32. Janca, J. Collection of Czechoslovak Chem. Commun., to be published.
33. Janca, J.; Pribylova, D.; Jahnova, V. Separation and dispersion in sedimentation field-flow fractionation. J. Liq. Chromatogr. **1987**, *10*, 767.

Received October 28, 2002
Accepted December 5, 2002
Manuscript 6001